Oxid Met (2008) 70:287–294
DOI 10.1007/s11085-008-9121-2

ORIGINAL PAPER

Effect of Mechanical Loading on the Oxidation Kinetics and Oxide-Scale Failure of Pure Ni

C. H. Zhou · H. T. Ma · L. Wang

Received: 18 December 2007 / Revised: 2 June 2008 / Published online: 5 November 2008

Abstract The oxidation kinetics and mechanism of oxide-scale failure of pure Ni oxidized under external static compressive and tensile loads were studied. The results showed that both types of mechanical loads accelerated the oxidation rate, but the effect was different for the two types. Compressive loading (CL) affected it by improving the plasticity of oxide scales, and tensile loading (TL) affected it by amplifying the compaction of the oxide–metal interface. As for the oxide-scale failure, CL can delayed cracking, TL accelerated brittle failure. The study analyzed the effect of external load on the oxidation kinetics and the failure mechanism of oxide scales.

Keywords Stress · High-temperature oxidation · Ni · Oxide-scale failure · Kinetics

Introduction

Nickel is one of the base metals in many of today's superalloys. The oxidation of pure nickel is one of the simplest examples of high-temperature oxidation. Therefore, many previous works were devoted to this model system. Though this simplicity is apparent, many parameters such as the metal purity, surface preparation, and orientation are known to affect the oxidation mechanism. These investigations mainly focused on the growth kinetics [1–4], oxide-scale morphology [3–6], or improvement of oxidation resistance by adding REEs [7, 8]. The oxidation kinetics obey the parabolic rate law at higher temperatures (>1000 °C), and lattice diffusion controls the growth of oxide scales. The oxide scales are usually faceted

C. H. Zhou · H. T. Ma (✉) · L. Wang
School of Materials Science and Engineering, Dalian University of Technology, Dalian 116024, People's Republic of China
e-mail: htma@dlut.edu.cn

resulting from the outward diffusion of nickel cations and minimization of surface energy [3–5]. It appears that the sub-parabolic rate law is followed at intermediate temperatures (700–1000 °C). Grain boundaries, dislocations, and defects play an important role in the diffusion process. The most specific feature of the oxide scales is a cellular or platelet-like morphology resulting from surface preparation, oxygen partial pressure, water–vapor concentration, or impurities [3–5]. The oxidation kinetics again conform essentially to a parabolic rate law at lower temperatures (<600 °C) [3].

In practical applications the oxide scales are stressed, either by externally applied loads, or by oxide-growth stresses or by thermal stresses. Oxide scales are prone to mechanical fracture. Several reviews [9–12] summarized the effect of internal or external stresses on the oxidation behavior, such as growth kinetics, oxide-scale failure, adhesion, or cohesion of scales. For pure nickel, Gaillet et al. [13] studied the creep behavior of a Ni single crystal and found that parallel cracks occurred at tensile loads greater than 10 MPa. Moulin et al. [14] found that creep and fatigue affected the scales thickness and oxygen diffusion, and macroscopic cracks were also revealed. Berger et al. [15] observed parallel cracks for loaded samples also. But the synergy between oxidation and stress application remains in question. This work investigated the oxidation behavior of Ni under static mechanical loads and analyzed the kinetics and oxide-scale failure.

Experimental Procedures

The nickel used in this investigation was in the form of plates. The chemical composition is given in Table 1. After cutting into 8 mm × 8 mm × l2 mm, and 2 mm × 8 mm × l2 mm dimensions, the specimens were then annealed by heating for 5 h at a temperature of 500 °C in vacuum, followed by cooling in air. Prior to oxidation, the specimens were abraded with SiC paper up to 2000 grade (2.5 μm) and ultrasonically cleaned in ethanol, then in acetone. At the end of each test, specimens were then observed by SEM on the surface and in cross-section. The static loading conditions will be presented with the results.

Results

Figure 1a shows the curves of weight gain as a function of load at different temperatures for 20 h in air. Both CL and TL accelerate the oxidation rate even though the curve for CL at 700 °C is irregular. Figure 1b shows the weight gain as a function of time for different mechanical loads at 700 °C in air, which shows that

Table 1 Chemical composition

Element	Ni	C	Si	S	Fe	Co
wt.%	99.9853	0.003	0.001	0.0006	0.008	0.001

with increasing load, the weight gains also increase except for one special case, Ni oxidized under 6 MPa TL, which has a similar weight gain as the one with no load. There might be a critical stress below which the load has no effect. The weight gains of CL samples are higher than TL ones for the same experimental conditions.

The surface morphologies of Ni oxidized under CL and TL are shown in Fig. 2, which shows different morphologies, i.e., a rumpled morphology under CL, while parallel cracks formed under TL.

Cross-sections of Ni oxidized under the two kinds of load are shown in Fig. 3, which exhibits two different morphologies. Discontinuous cavities formed at the oxide–metal interface under CL, whereas cavities accumulated at the oxide–metal interface even transgranular cracks formed in the oxide scales under TL.

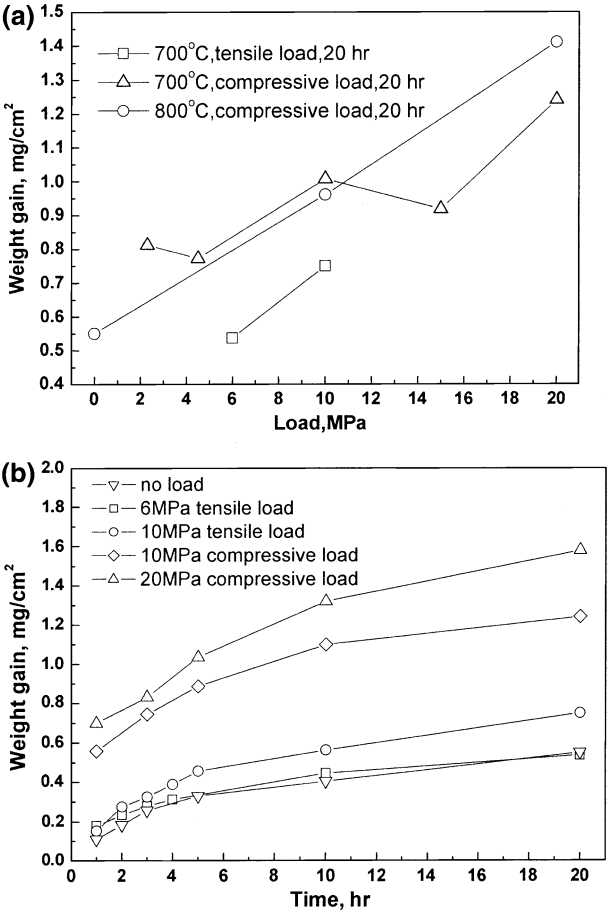

Fig. 1 Oxidation kinetics curves of pure Ni (**a**) the weight gain as a function of load for oxidation of Ni under TL and CL at 700–800 °C for 20 h and (**b**) the weight gain as a function of time for oxidation of Ni under TL and CL at 700 °C for 20 h

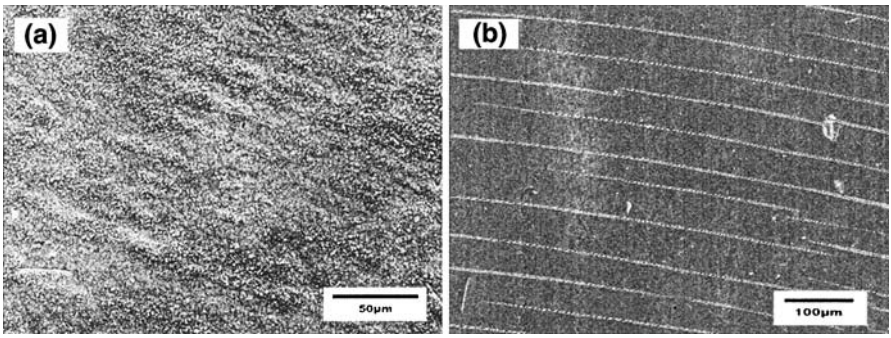

Fig. 2 Surface morphology of pure Ni oxidized under CL and TL. (**a**) Surface morphology of Ni oxidized at 800 °C under 20 MPa CL for 20 h and (**b**) surface morphology of Ni oxidized at 700 °C under 10 MPa TL for 20 h

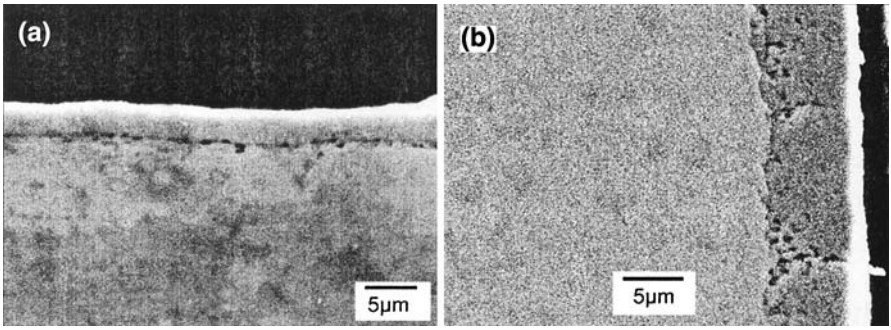

Fig. 3 Cross-section of pure Ni oxidized under TL and CL. (**a**) Cross-section of Ni oxidized at 700 °C under 10 MPa CL for 20 h and (**b**) cross-section of Ni oxidized at 700 °C under 10 MPa TL for 20 h

Discussion

Oxidation Kinetics

Literature concerning the oxidation kinetics of alloys oxidized under stress is sparse, but it is known that mechanical stresses can accelerate oxidation rates. Stresses affect grain-boundary diffusion and make excessive vacancies accumulate at the oxide–metal interface, thus the diffusion behavior of cations might change. On the other hand, the stress state near the oxide–metal interface would change by the application of mechanical stresses. It was found [16] that 1% tensile strain rate accelerated the oxidation rate of IN800H. Rolls et al. [17] also found that external stress accelerated oxidation rates suggesting that creep played a role. Richmond et al. [18] suggested that there was a critical value above which external stress affected the oxidation rate, but the mechanism was still ambiguous. In the present study, it was found that stress had no effect on the oxidation rate of Ni at 700 °C under 6 MPa TL.

The mechanisms of the effects of CL and TL on the oxidation kinetics are different. Rolls et al. [17] suggested the increasing oxidation rate might be linked with the possibility of there being a greater vacancy flux injected into the substrate. A decrease in the vacancy supersaturation at the scale–metal interface would favor an increase in the oxidation rate. The cavities formed at the scale–metal interface under CL, which would decrease the oxidation rate. In fact, because the porous zone extends over some distance, activity gradients in the scale provide partial pressure gradients in the void space. The metal gases in the porous inner scale permit and support continued scale growth. In addition, the stress affects the oxide–gas interface stress distribution near grain boundaries and increases the diffusion rate of Ni ions, thus the oxidation rate of Ni is accelerated. Also, the plasticity of oxide scales is increased due to the effect of load on deformation near grain boundaries, which reduces fracture and the spalling of oxide scales. Diffusion creep increases the oxidation rate in the form of decreasing the vacancies concentration at the scale–metal interface under TL. Vacancies are prone to incorporation into the metal with annihilation at grain boundaries or dislocations under TL, which permits the inherent chemical bonds to maintain intimate contact at the scale–metal interface. Thus the reduced diffusion path deduces an increasing of cation diffusion, and the oxidation rate is increased. The weight gains under CL are higher than that under TL, which is related to different microstructure under both stresses, as shown in Figs. 2 and 3. The oxide scales maintain their integrity under CL, while cracks generate under TL. Perhaps tensile strains above 1% or a tensile stress above some critical value, provide no healing at the crack regions [19], thus the weight gains per unit area are lower.

Oxide-Scale Failure

The effect of stresses on oxide-scale failure is focused mainly on growth stresses and thermal stresses. Growth stress is due to the volume change of oxide scales and consumable metals. Several models have been proposed, such as oxide scales having a PBR $>$ l, and for accommodation of new oxide formed at the oxide–metal interface by metal vacancies, which suggest that compressive stresses develop in the oxide scales [10]. Thermal stresses develop in both the oxide and substrate during temperature changes as a result of a mismatch between the thermal-expansion coefficients of oxide and metal, and the oxide layer experiences a compressive stress. Though studies on the oxidation behavior under external stresses are scarce, some models have been proposed. Nagl et al. [9] reviewed the proposed failure mechanisms and models of oxide scales under tensile and compressive loads. Two types of classical oxide-scale failures were proposed by Evans [20], i.e., strong interface and weak oxide (type I), weak interface and strong oxide (type II). In the present work, the oxide scales failure under TL belongs to type I and that under CL belongs to type II.

Gibbs et al. [21] analyzed the development of micro-channels above interfacial voids, which attempted to explain the effect of stresses on oxide-scale failure as illustrated by Fig. 4. The difference between the oxygen pressure in the voids and the air pressure drives the cation diffuse, resulting in the generation of micro-cracks

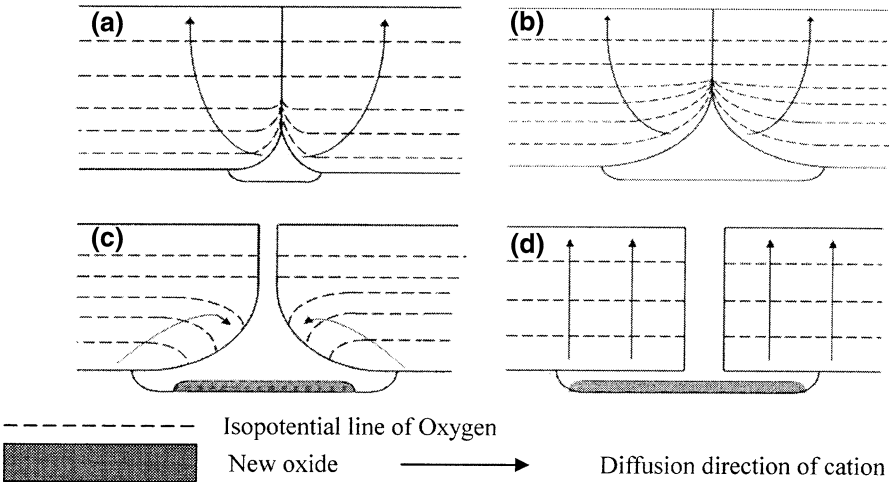

Fig. 4 Sketch of growth of cavities and microchannels development above them

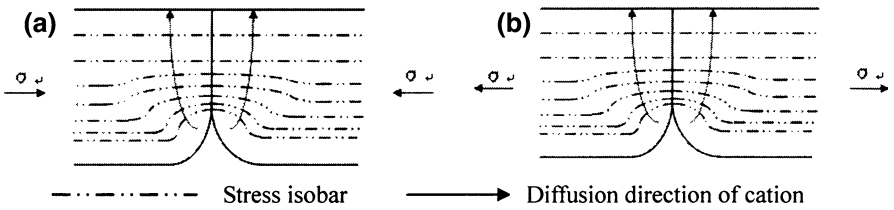

Fig. 5 Sketch of stress distribution at defect (**a**) CL and (**b**) TL

with increasing time. Furthermore, when a CL is applied, vacancies are accelerated to coalescence at the oxide–metal interface, cavities develop, and stress concentrations generate near the cavities, as shown in Fig. 5a. When subjected to a TL, stress concentrations are also generated near gain boundaries within the scales, as shown in Fig. 5b. According to the Nabarro-Herring creep model [22], the creation of a vacancy at the face acted on by the compressive stress is equivalent to a replacement of an atom from the inside of the crystal to its face. Thus tensile stress accelerates diffusion of vacancies into the substrate. On the contrary, compressive stress induces accumulation of vacancies at the scale–metal interface. So CL weakens the strength of the scale–metal interface, and the scales are prone to separate from the substrate. TL maintained intimate contact at the scale–metal interface, and the adhesion of scales is improved.

Figure 6 shows classic oxide-scale failure under CL and TL. Schütze [23] suggested that buckling under CL influences the morphology because of oxide-scale plastic deformation by creep at high temperatures. Although the scales show good plasticity and no cracks form, there is no guarantee that the protective effect would last indefinitely. Especially for cavities formed at the oxide–metal interface, where internal oxidation would occur. However, the internal stress within scales can

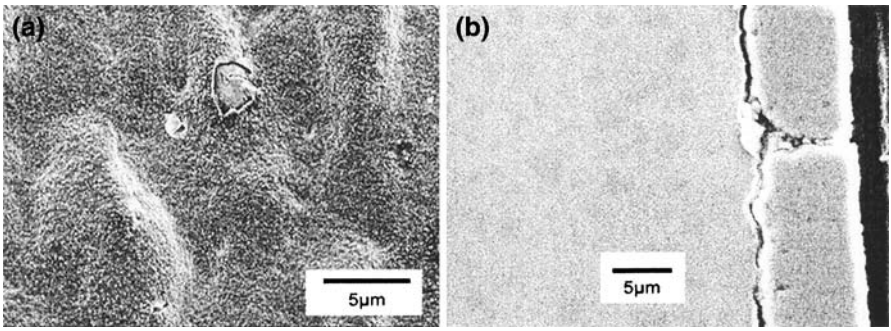

Fig. 6 SEM micrographs of pure Ni oxidized under CL and TL. (**a**) Surface morphology of Ni oxidized at 800 °C under 10 MPa CL for 20 h and (**b**) cross-section of Ni oxidized at 700 °C under 10 MPa TL for 20 h

decrease at delaminated parts or cavities. So we can say that the plasticity of scales is improved. Such an array of cracks formed under TL has been observed by many authors [13–15, 24], it appears that when the applied stress exceeds a critical stress for oxide failure by cracking: $K_{1C} = \alpha\sigma_c\sqrt{\pi a}$ where K_{1C} is the critical stress-intensity factor, σ_c is the critical stress, a is the size of an equivalent composite defect, and α is the correction factor) [24]. With K_{1C} and σ_c being constant for a given oxide scale, only the defect size varies, thus after exceeding the critical size, cracks would be generated. Figure 3b shows the crack source at a microcrack where cavities accumulate and increase the defect size, thus the strength of oxide scales is weakened.

Conclusions

(1) Stress affects the diffusion of cations near cavities at the oxide–metal interface and increases the internal oxidation rate under compressive loads, whereas tensile loads induced vacancy flux injection into the substrate and strengthened the oxide–metal interface adhesion. Both tensile and compressive stresses accelerate the oxidation rate of Ni.

(2) A rumpled morphology forms owing to oxide-scale plasticity under compressive loads. The oxide scales cracks beyond some critical value under tensile loads, such value is approximately 10 MPa at 700 °C.

Acknowledgment This work was supported by Chinese National Natural Science Foundation (No. 50601004).

References

1. R. Peraldi, D. Monceau, and B. Pieraggi, *Oxidation of Metals* **58**(3/4), 275 (2002).
2. A. M. Huntz, M. Andrieux, and R. Molins, *Materials Science and Engineering* **A415**, 21 (2006).
3. R. Haugsrud, *Corrosion Science* **45**, 216 (2003).

4. F. Morin, L. C. Dufour, and G. Trudel, *Oxidation of Metals* **37**(1/2), 39 (1992).
5. R. Peraldi, B. Pieraggi, and D. Monceau, *Oxidation of Metals* **58**(3/4), 249 (2002).
6. D. Caplan, M. J. Graham, and M. Cohen, *Journal of Electrochemical Society* **119**(9), 1205 (1972).
7. R. Haugsrud, *Corrosion Science* **45**, 1289 (2003).
8. F. Czerwinski, Ph.D. thesis, McGill University, Montreal, 1997.
9. M. M. Nagl and W. T. Evans, *Journal of Materials Science* **28**, 6247 (1993).
10. H. E. Evans, *International Materials Reviews* **40**(1), 1 (1995).
11. J. Robertson and M. I. Manning, *Materials Science and Technology* **6**, 81 (1990).
12. M. Schütze, *Materials Science and Technology* **4**, 407 (1988).
13. L. Gaillet, M. Viennot, P. Berger, and G. Moulin, *Materials Science and Engineering* **A332**, 382 (2002).
14. G. Moulin, P. Arevalo, and A. Salleo, *Oxidation of Metals* **45**(1/2), 153 (1996).
15. P. Berger, G. Moulin, and M. Viennot, *Nuclear Instruments and Methods in Physics Research* **B130**, 717 (1997).
16. M. F. Stroosnijder, V. Guttmann, R. J. N. Gommans, and J. H. W. De Wit, *Materials Science and Engineering* **A121**, 581 (1989).
17. R. Rolls and M. H. Shahhosseini, *Oxidation of Metals* **18**, 115 (1982).
18. J. Richmond and H. Thornton, in *Oxidation of Experimental Alloys*, EADC Tech. Rep. 58–164, Part l, National Bureau of Standards, June 1958.
19. M. Schütze, *Oxidation of Metals* **25**(5/6), 409 (1986).
20. H. E. Evans, *Materials Science and Technology* **4**, 415 (1988).
21. G. B. Gibbs and R. Hales, *Corrosion Science* **17**, 487 (1977).
22. F. R. N. Nabarro and C. Herring, in *Creep in Metallic Materials: Dusional Creep*, ed. J. Cadek (Academia Prague, Czechoslovakia, 1988), p. 208.
23. M. Schütze, *Materials Science and Technology* **6**, 32 (1990).
24. L. Gaillet, S. Benmedakhne, A. Laksimi, and G. Moulin, *Journal of Materials Science* **38**, 1479 (2003).